

Dependence of morphology on miscut angle for Si(111) etched in NH_4F

Joseph Fu, Hui Zhou, John Kramar, and Richard Silver^{a)}

*Precision Engineering Division, National Institute of Standards and Technology,
Gaithersburg, Maryland 20899*

Satoshi Gonda

*Advance Semiconductor Research Center, AIST Tsukuba Central3, 1-1 Umezono 1-Chome, Tsukuba,
Ibaraki 305-8563, Japan*

(Received 17 January 2003; accepted 4 March 2003)

Hydrogen-terminated silicon surfaces are important and commonly used in several nanotechnology applications. A significant obstacle to their widespread use has been the repeatable preparation of large, flat surfaces. Using scanning probe microscopy, we have examined the surfaces of several vicinal Si(111) samples, with miscut angles ranging from 1.1° to 0.01° , produced by etching in a NH_4F aqueous solution. Although the miscut angle sets the nominal terrace width, we have found that with wet chemical etch processing, as the vicinal angle decreases, the terrace width increases only to a maximum of ~ 200 nm, limited by the etching anisotropy. The result is that for miscut angles below a critical angle, the surface roughness actually *increases*. © 2003 American Institute of Physics. [DOI: 10.1063/1.1569426]

For nanomanufacturing to evolve as an industry, measurement, calibration, and fabrication techniques must become more robust and repeatable. An essential enabling technology at this scale is the preparation of atomically flat and ordered surfaces. Silicon is a highly desirable substrate for this work because of its widespread usage in semiconductor manufacturing. One difficult challenge several research groups have encountered in attempting to use Si in nanotechnology applications has been in finding a robust method for the repeatable preparation of large, ordered, flat surfaces.

Using conventional high-temperature annealing processing, one can produce large, atomically ordered planes on Si, on which atomic resolution imaging is possible with scanning tunneling microscopy. Although these surfaces are possible candidates for nanofabrication and measurement in some applications, in cases where the surfaces are patterned, the high processing temperatures cause significant damage to feature shape and integrity. An alternative is wet chemical etch processing which can produce high-quality atomically flat Si(111) surfaces without the requirement of high temperature.¹ The etching process results in hydrogen-terminated Si (1×1) surfaces that are quite stable in an ambient environment.² The hydrogen termination can be locally removed through electron stimulated desorption,^{3,4} making it possible to fabricate nanoscale artifacts using a scanning probe microscope.

Although most research groups working in this area use a common Radio Corporation of America-type⁵ preclean followed by a HF etch, the details vary widely. Earlier, it was found that flatter surfaces can be produced by increasing the pH of the etchant solution,⁶ so most researchers moved from using dilute HF to using a 40% NH_4F solution. Later, it was discovered that reducing the dissolved oxygen in the solution further reduces the appearance of triangular etch pits.⁷⁻⁹ Other parameters have also been examined including the

angle and direction of vicinal miscut,¹⁰ the doping type and level,¹¹ and more recently, the beneficial effect of a sacrificial mechanically roughened area.¹² Modeling studies have also been performed to elucidate the relative etching rates.¹³ Although there are many reports of producing defect free surfaces, and some have demonstrated atomically resolved imaging,⁸ there has been much variability of success, and some reported results have been difficult to repeat elsewhere. To better understand the wet etching process and to develop more repeatable procedures, we have systematically studied various etching conditions on control wafers with several different miscut angles. With close attention paid to the preparation details, the measurement data repeated consistently from sample to sample. We have found that the wafer miscut angle plays a critical role in the determination of the final morphology of the H-Si(111) surfaces.

In experiments, several Si(111) samples from different wafers were used, including both *n* and *p* type, with various miscut angles ranging from 1.1° to 0.01° . The samples were all cleaned as follows: The samples were placed in a 4:1 mixture (by volume) of 98% H_2SO_4 :30% H_2O_2 at 40°C for 30 min. This was followed by a twice repeated 10 min ultrasonic rinse in highly purified distilled water¹⁴ (>18 M Ω cm). This step is intended to remove any organic residues. The samples were then dipped in 2% HF solution for 1 min to remove the native oxide on the surface, followed by an ultrasonic rinse in ultrapure water for 10 min. Subsequently, the samples were placed in a 5:1:1 solution of H_2O :35% HCl:30% H_2O_2 ($\text{pH}\cong 0.2$) at 80°C for 10 min to remove metallic contaminants and to reoxidize the surface. This was again followed by two 10 min ultrasonic rinses in ultrapure water. After this cleaning procedure, an atomic force microscope (AFM) image showed that the root-mean-square roughness, R_q , had slightly increased from 0.12 nm to 0.13 nm. All samples were processed with these same cleaning procedures.

The samples were then submerged in a 40% by weight

^{a)}Electronic mail: silver@nist.gov

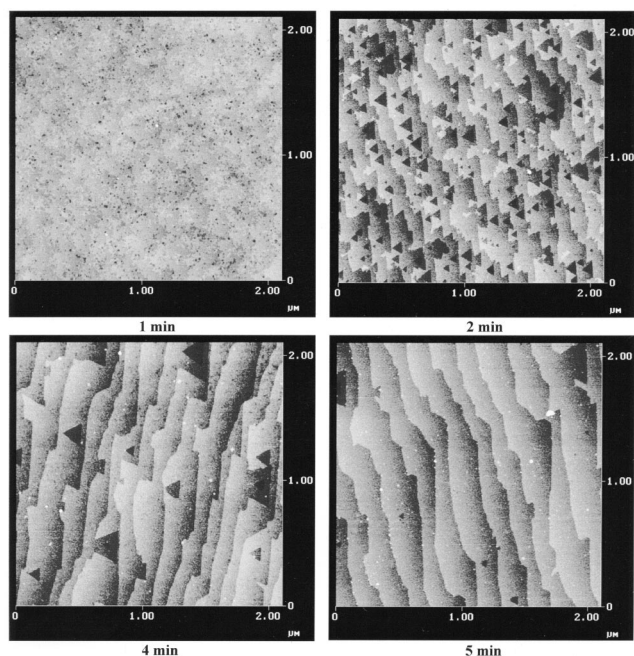


FIG. 1. A set of AFM images of Si(111) surfaces after etching in NH_4F for various times as indicated. Each image size is $2.1 \mu\text{m}$ by $2.1 \mu\text{m}$. The sample was 0.15° off the (111) plane.

aqueous NH_4F solution for varying etching times ranging from 1 min to several hours. The NH_4F solution was sparged (bubbled) with Ar gas for 45 min to displace the dissolved oxygen prior to immersing the samples. Finally, the samples were rinsed with ultrapure water for 5 s to 10 s after etching. We have also experimented with different sparging gases, such as N_2 , O_2 , and ambient air. Both the Ar- and N_2 -sparged solutions resulted in samples having significantly fewer triangular etching pits than those etched with nonsparged solutions. There was no beneficial effect from the O_2 or ambient air sparging.

Since the average terrace width is a direct function of the wafer miscut angle, these angles were confirmed by AFM measurements following high-temperature annealing in UHV. For an ideally terminated surface, the relationship between the miscut angle, θ , and average step spacing, s , is described by $s = (0.314 \text{ nm}) / \tan \theta$, where 0.314 nm is the height of a single Si(111) bilayer step.

Figure 1 shows a set of images taken from a Si(111) sample with a miscut angle of 0.15° . The samples were etched in a NH_4F solution for varying amounts of time as indicated. In the early stages of etching, both the triangular etch pits and the step-terrace structures exist, with many small etch pits covering the surface. As the etching time is increased, the number of pits decreases while their average size increases. The etch pits merge with each other, leaving exposed points which are more rapidly etched, tending toward straight step edges. Eventually, the surface evolves into its steady-state staircase arrangement of step-terrace structures with very few remaining etch pits. It appears that the initial high density of etch pits is due to the previous processing having left a high density of reactive sites that are more easily attacked by the etchant than the uniform hydrogen-terminated terrace sites that develop later. Although these reactive sites may be remnants of the mechani-

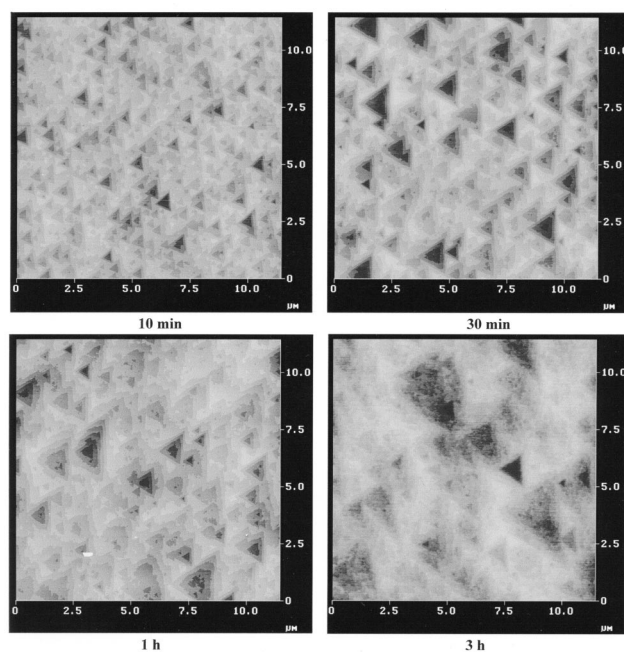


FIG. 2. A set of AFM images of Si(111) surface after etching in NH_4F aqueous solution for various times as indicated. Each image size is $11.5 \mu\text{m}$ by $11.5 \mu\text{m}$. The Si(111) sample was miscut with 0.015° off the (111) plane.

cal polishing process, in view of the surface removal that has already occurred during the cleaning process and the uniform distribution of the etch pits, it is more likely that they are due to broken bonds caused by the immediately preceding surface oxidation. This explanation is further supported by the observation of Wade and Chidsey⁷ that immersing a previously etched, uniform, terraced, and H-terminated sample into O_2 -containing etchant results in the reappearance of many small etch pits.

To investigate further, we prepared Si(111) samples with very small miscut angles: *n*-type 0.05° and *p*-type 0.015° . We used etching times ranging from 10 min to 3 h. Results for the 0.015° sample are shown in Fig. 2. For these samples, the size of the triangular pits increased with the etching time as expected; however, the uniform step-terrace features never formed, even after 3 h of etching. The surface roughness over large areas increased relative to the surfaces with a higher miscut angle due to the lack of a uniform distribution of steps and terraces. This difference was confirmed by additional experiments in which identical solutions and etching times were used for samples with the larger (0.15°) and the smaller (0.05° and 0.015°) miscut angles. The resulting surface morphologies were quite different. The larger miscut angle surface had uniformly spaced single atomic steps, while the other had large triangular etching pits, the only difference in preparation conditions being the wafer miscut angle.

The steady-state end-point morphology of the surfaces with different vicinal miscut angles can be understood in terms of the relative etching rates for the distinct surface sites as described by Flidr and co-workers.¹³ The $\langle 11\bar{2} \rangle$ step edges (those oriented normal to the $\langle 11\bar{2} \rangle$ directions) etch more slowly than the $\langle \bar{1}\bar{1}2 \rangle$ step edges. This is the reason for the triangular shape of the etch pits. The etch rate of these $\langle 11\bar{2} \rangle$ step-edge sites in the lateral direction, \mathbf{L} , is in turn much

faster than the etch rate for the extraction of a terrace site atom in the vertical direction, V . As a single layer triangular etch pit begins to expand, more and more of the underlying surface is exposed. Eventually, an etching pit nucleates in this second layer. Statistically, this nucleation site is most likely to be located near the center of the first layer etch pit since these sites have had the longest exposure to the etchant. Also, a local depletion of the reactive entity is likely in the solution near the propagating step edge.¹⁰ The average terrace width within a multilevel triangular etch pit is a measure of the ratio between L and V . From our data, a typical terrace width within an etch pit is approximately 250 nm. The lattice spacing in the $\langle 111 \rangle$ direction is about 314 pm, so an approximate $L:V$ ratio for our etching solution is 800:1.

As two adjacent triangular etch pits grow, they eventually collide with one another resulting in an intersection point along their now common step edge. These intersection sites are more easily attacked by the etchant solution than the straight $\langle 11\bar{2} \rangle$ step edges and are soon rounded, eventually collapsing and straightening and leaving behind the more stable $\langle 11\bar{2} \rangle$ step edges.

For vicinal surfaces with moderate miscut angles, one side of an expanding etch pit will eventually penetrate the advancing step edge, causing the pit to merge with the next lower terrace. The points that are formed in the step edge will etch more quickly than the $\langle 11\bar{2} \rangle$ edges, as just discussed, until a uniform $\langle 11\bar{2} \rangle$ step edge results. These uniform step edges will flow across the surface at a constant rate L . Etch pits may initiate on the terraces, but if the average terrace width (given by the miscut angle) is small, relative to the $L:V$ ratio, these will be infrequent events; any etch pits that do form will not grow very large before they are subsumed into the advancing step edge.

For vicinal surfaces with very small miscut angles, the etching pits are not generally able to reach and penetrate the adjacent step edge before another etch pit is initiated within them. With very small miscut angles, and the limited $L:V$ ratios of the etchant solution that bound the maximum average terrace width, etch pits which are several layers deep may form. So, for very small miscut angles, even though the individual terraces are generally wider than on surfaces with larger miscut angles, when taken on a more macroscopic level, the surface is less uniform and has greater surface roughness. With the Ar-sparged, 40% NH_4F solutions, the optimal miscut angles for forming etch-pit free surfaces seems to be around 0.1° . We emphasize that it is the $L:V$ ratio that limits the terrace width. Evidently, lowering the $p\text{H}$ or allowing O_2 to remain in the etchant solution decreases

this ratio either by increasing the terrace etch rate⁷ or by decreasing the step-edge etch rate.⁹ Since it is preferable for our intended applications to produce large terraces, it would be desirable if we could modify the etchant to further increase the $L:V$ ratio.

We have shown that for given etching conditions, the etching time and the miscut angle of the Si crystal determine the morphology of the resulting surface. Initially, the surface is covered with small triangular etch pits, which then grow and merge into larger pits. For limiting etching times, smaller miscut angles will result in wider terraces up to the maximum allowed by the selective etch ratio of the etchant; smaller angles beyond this limit will lead to a higher surface roughness because of the formation of multilayer etch pits. Optimally flat surfaces can be formed by choosing the correct miscut angle for the given etching solution, and by ensuring adequate etch times. Understanding these results has significantly improved our ability to reproducibly prepare ordered step-and-terrace hydrogen-terminated Si(111) surfaces.

The authors would like to thank Dr. Mineharu Suzuki at NTT for providing 0.015° miscut sample. This work was partially supported by the Nanomanufacturing Program of the NIST Manufacturing Engineering Laboratory and by the NIST Office of Microelectronic Programs.

¹G. S. Higashi, R. S. Becker, Y. J. Chabal, and A. J. Becker, *Appl. Phys. Lett.* **58**, 1656 (1991); R. S. Becker, G. S. Higashi, Y. J. Chabal, and A. J. Becker, *Phys. Rev. Lett.* **65**, 1917 (1990).

²Y. Kim and C. Lieber, *J. Am. Chem. Soc.* **113**, 2333 (1991).

³M. Schwartzkopf, P. Radojkovic, M. Enachescu, E. Hartmann, and F. Koch, *J. Vac. Sci. Technol. B* **14**, 1336 (1996).

⁴J. A. Dagata, J. Schneir, H. H. Harary, C. J. Evans, M. T. Postek, and J. Bennet, *Appl. Phys. Lett.* **56**, 2001 (1990).

⁵W. Kern and D. A. Puotinen, *RCA Rev.*, 187 (1970).

⁶P. Jakob and Y. J. Chabal, *J. Chem. Phys.* **95**, 2897 (1991).

⁷C. P. Wade and C. E. D. Chidsey, *Appl. Phys. Lett.* **71**, 1679 (1997).

⁸H. Sakaue, S. Fujiwara, S. Shingubara, and T. Takahagi, *Appl. Phys. Lett.* **78**, 309 (2001).

⁹H. Fukidome and M. Matsumura, *Appl. Surf. Sci.* **130**, 146 (1998).

¹⁰G. J. Pietsch, U. Köhler, and M. Henzler, *J. Appl. Phys.* **73**, 4797 (1993).

¹¹M. Ramonda, P. Dumas, and F. Salvan, *Surf. Sci. Lett.* **411**, L839 (1998).

¹²P. Allongue, C. H. de Villeneuve, S. Morin, R. Boukherroub, and D. D. M. Wayner, *Electrochim. Acta* **45**, 4591 (2000).

¹³J. Flidr, Y.-C. Huang, T. A. Newton, and M. A. Hines, *J. Chem. Phys.* **108**, 5542 (1998); J. Flidr, Y.-C. Huang, and M. A. Hines, *J. Chem. Phys.* **111**, 6970 (1999).

¹⁴Nanopure Infinity System from Barnstead/ThermoLyne Corporation. Certain commercial products are identified in this article in order to specify the experimental procedure adequately. Such identification does not imply recommendation or endorsement by NIST, nor does it imply that the materials or equipment specified are necessarily the best available for the purpose.